

# Characterization of High-fidelity Color Printing Devices Based on both Multispectral and Broadband Approaches

Lo, Mei-Chun<sup>\*</sup>, Chen, Chang-Lang<sup>#</sup> and Hsieh, Tsung-Hsien<sup>#</sup>

<sup>\*</sup>Department of Information Management, Shih Hsin University, Taipei, Taiwan

<sup>#</sup>Department of Graphic Communication Arts, National Taiwan University of Arts, Taipei, Taiwan

## Abstract

*In recent years, for printing qualities, it's important and valuable to bring more accurate and colorful reproductions to cope with the tremendous development of optoelectronic age. Thus, for the gamut, the term of "High-Fidelity (Hi-Fi) Color Printing" is the meaning of using the extra colorants to advance the printability of color printers and it is also called "Multi-color printing". Two directions have been abidingly suggested and induced for multi-color printing in many related papers. Firstly, with the same hues and different concentrations as standard inks, light magenta ( $L_m$ ) and light cyan ( $L_c$ ) are always used to be the extra colorants (e.g. CMYKL $_m$ ) to optimize the smoothness of image detail from high light to shadow. In the second direction, with different hues, the extra colorants usually offer the opportunity to standard process to extend the printable gamut. This idea, for the most part, is used to compensate for the gamut of the secondary colors, e.g., CMYKRGB, CMYKOG or CMYKV sets. Indirectly, one can well imagine, then, it also augments the stability of tertiary colors. Additionally, as metamerism issue concerned under all possible illumination conditions happened in real world, colorimetrically color matching of colors is not necessarily correct and acceptable results for an accurate color reproduction. Therefore, the only solution, to achieve the optimally requirement of color-matching independent of the illuminants, would be the reconstruction of spectral reflectance of every color interest. Therefore, the aim of this research was to derive the printing device characterization modules which can be used in the high-fidelity multi-color*

*printing processes and also using the multispectral approaches. The IT8.7/4 test target was used in the preliminary stage of derivation. Two types of the multispectral (i.e. narrowband) and the broadband were developed in this study. Both broadband and multispectral device characterization models were all constructed including both transforms of forward and reverse processes. Both of the broadband-based and the spectrally-constructed models used 2<sup>nd</sup>-order and 3<sup>rd</sup>-order polynomial regression equations, and all applying singular value decomposition method (SVD). They were referred as 3<sup>rd</sup>-SVD-MS and 2<sup>nd</sup>-SVD-BB respectively in this study. A color difference formula of CIEDE2000 (i.e.  $\Delta E^*_{00}$ ), via the evaluation of the IT8.7/4 target as a test data set, was used to compare the predictive performance between two models, in both the forward and the reverse transforms derived.*

## Introduction

As known, both the quality of the illuminant and the nature of the objects contribute towards the color seen. Also, it is clear, as metamerism issue concerned under all possible illumination conditions happened in real world, that colorimetrically correct results are not necessary for a color reproduction to be acceptable. Therefore, it is the only actual solution in practice to carry out spectral color reproduction, which provides a detailed description of color properties of the color-sample surface of interest in terms of its spectral reflectance or transmittance curve, across color-imaging media. That is to define each spectral color by the wavelength of its light. Hence, suppose every color of an image reproduced has the same spectral reflectance curve as the one of the original

image, then, it can produce the physically identical effect for both the original and the reproduced images. Both the original and the reproduction will always look alike in identical circumstances (e.g. viewed in the same surroundings), although of course they will both change colors as the illuminant is changed.

From above discussions, it is clear that the reproduction of the spectral reflectance curve of every color of image considered can help to solve out metamerism problem in the application of any color reproduction system. However, to achieve this objective mentioned, there is another important problem also needed to be addressed. That is the issue of different color gamuts of the imaging devices. In recent years, for printing qualities in Graphic Arts, it's important and valuable to bring more accurate and colorful reproductions to cope with the tremendous development of optoelectronic age. Although the 4-color CMYK printing process is the state-of-the-art technology, its chromaticity gamut is still restricted when compared with the gamuts of displays (used for soft-proofing) or real dyes. Thus, in addition to the use of spectral approach, it is desirable and practicable to achieve the optimally requirement of color-matching independent of the illuminant, but also by considering the use of High Fidelity of multi-color printing process.

The term of "High-Fidelity (Hi-Fi) Color Printing" means that the use of extra colorants with the conventional CMYK primaries would extend color gamuts, approaching display and film gamuts. Therefore, one approach to obtaining more colorful images is to augment a set of process CMYK inks with traditional spot inks which increase the attainable color gamut. Furthermore, in CMYK process, it usually averts these graphic products from the problems of "moiré" or "rosette" or by taking advantage of different angles to set the overprint positions of these four color screens. But, in the process with more than 4-color inks, there aren't any screen-angle sets can satisfy such situation. Therefore, it's necessary to adopt a frequency modulation (FM) technology in the color separation process.

Between many optical problems (such as first-surface reflection, multiple internal reflections, opacity, ink

trapping, back-transfer effects, spectral characteristics, halftone structure, and light scatter in the paper (Yule 1967), rendering of image detail and colorfulness of secondary colors are always decreased when printing devices overprint the standard process inks (C, M, Y, K). Therefore, original images are separated using "Multi-Color Separation Approaches" (e.g., Pantone® Hexachrome system) to reduce the graininess and to extend the gamut for reproductions by multiple-ink sets. Generally, 5-8 color separations are the most usages, and each multi-color set usually has its own purposes in Hi-Fi color printing application.

Two directions have been abidingly suggested and induced for the separations in many related papers. Firstly, with the same hues and different concentrations as standard inks, light magenta (Lm) and light cyan (Lc) are always used to be the extra colorants (CMYKLCm) to optimize the smoothness of image detail from high light to shadow (Son *et al.* 2005). In the second direction, with different hues, the extra colorants usually offer the opportunity to standard process to extend the printable gamut (Ostromoukhov 1993). This idea in Graphic Arts, for the most part, is used both to compensate for the gamut and to achieve the lighter or better hue, of some saturated colors (e.g. by using CMYKRGB, CMYKOG or CMYKV sets). Those colors in question are such as orange, violet, certain reds, blue, purple and certain greens, which cannot be reproduced by conventional CMYK printing. Indirectly, one can well imagine, then, it also augments the stability of tertiary colors. A schematic of Hi-Fi color gamut of CMYKRGB studied here is shown in Figure 1.

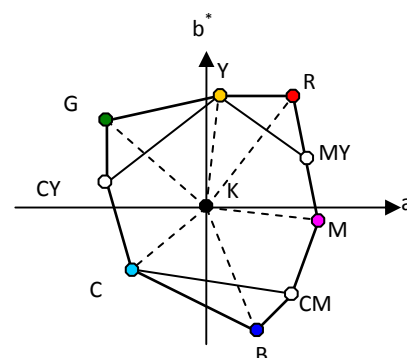


Figure 1. Add extra R, G, B colorants to extend the gamut achieved with standard CMYK printing process.

With the descriptions given above, for the graphic quality, Hi-Fi color printing not only enables the advance of the density range, resolution and the rendering of details but also profit the representable gamut. For the recessionary business, high-end market is the only niche to find the real direction of new enterprising type. As a matter of fact, for the production cost, only a few industries apply Hi-Fi color procedures to be the arch-production line. Also, for the technical staffs of printing concerns, these techniques are even more difficult to be generally explored now. However, the reasons given above stimulate many motivations for this category to be researched and discussed.

Therefore, by taking two kernels of the matters of both “metamerism” and “gamuts” in mind, the intent of this research was to derive universally well-performing Hi-Fi multicolor printing device characterization model, which explored both feasible approaches of FM screening separation and/or multi-spectra (i.e. color-matching independent of the illuminant) to process the color complex-images. The printing device characterization here is defined as the derivation of colorimetrically color-to-ink transform to determine the conversion between device-dependent data (for instance CMY or CMYK) and device-independent data (i.e. CIE XYZ/L\*a\*b\*) via the provision of training data (here IT8.7/4 was used).

#### Subdivision Approach and Modeling Color Behavior for 7-ink CMYKRGB Printing Process

The extension of the printing process by introducing additional basic colors RGB to CMYK, using FM screening, was proposed in this study. The heptatone (7-color) CMYKRGB process, as shown in Figure 1, extends the color gamut beyond what can be achieved in the conventional CMYK printing system. The approach carried out is based on the scheme suggested by Harold Boll (1993). The superset CMYKRGB was subdivided into 7 groups of 4-ink subsets (see table 1), each containing 3 chromatic inks and black ink. Six groups of 4-color subsets, except for CMYK subset, represent six adjacent and overlapping subgamuts in the supergamut of the 7-ink CMYKRGB color space. Each 4-ink set was then characterized as strictly as a

conventional CMYK ink set. This approach results in the production of an inktable wherein every color of images reproduced is inked with a maximum of 4inks.

As known in the traditional CMYK printing process, a colorimetric equivalency is present between the CMY and black inks. Hence, a GCR (Gray Component Replacement) approach is technically used to remove the third contaminant component (i.e. gray component) produced from a combination of three primary inks CMY, and replace it with black ink instead. Similarly in theory, following the work derived previously (Lo *et al.* 1997, 1998), a KCR (Key Component Replacement) algorithm was also applied in each of subgamuts in this work. It refers, e.g. in RKYM and KRYG subgamuts as listed in Table 1, to reduce key components R and K respectively (which are produced using paired inks of M & Y, and R & G respectively), and substitute them with colorimetrically corresponding equivalent amounts of red (R) and black (K) inks respectively. Thus, the characterization of 7-ink printing process in this study was to derive modeling method, by measuring a number of colors in the IT8.7/4 test target produced using each subset of 4-ink grouping, to define the transform between color (i.e. device-independent data) and ink (i.e. device-independent data).

Table 1. Seven subsets of 7-ink color separation

Dominant Ink	Subgamut	Key Component
Black	CMYK	Black
Cyan	KGCB	Black(K)
Magenta	KBMR	Black(K)
Yellow	KRYG	Black(K)
Red	RKYM	Red
Green	GKYC	Green
Blue	BKMC	Blue

#### Device Characterization Models

As explained above, this research considered two kernels of the matters of both “metamerism” and “gamuts” in mind. Therefore, two approaches of multispectral and broadband, used in the printing device characterization, were explored. Both models, using multispectral and broadband approaches, numerically respectively applied both the 3<sup>rd</sup>-order.

Table 2. Polynomial equations used in the derivation of 7-ink printing device characterization (for forward transform).

Orders	Parameters	Matrix Length	Polynomial Equations
n <sup>Order</sup> -SV D Equation	m	$(\sum_{i=0}^n H_i^m) + 1$	$\sum_{j=1}^{C_n^{m+i}} a_j n^{Order} (m) + (n-1)^{Order} \sum_{j=C_i^{m+i}+1}^{C_n^{m+n} + C_{n-1}^{m+n-1} \dots} a_j (m) + \dots + 1$
3 <sup>rd</sup> -SVD Equation (BB)	$D_{rc}$ $D_{gm}$ $D_{by}$	$(\sum_{i=0}^3 H_i^3) + 1 = 20$	$\sum_{j=1}^{C_3^5} a_j 3^{rd} (D_{rc}, D_{gm}, D_{by}) +$ $\sum_{j=C_3^5+1}^{C_3^5+C_3^4} a_j 2^{nd} (D_{rc}, D_{gm}, D_{by}) +$ $\sum_{j=C_3^5+C_3^4+1}^{C_3^5+C_3^4+C_3^3} a_j 1^{st} (D_{rc}, D_{gm}, D_{by}) + 1$ $\sum_{j=1}^{10} a_j 3^{rd} (D_{rc}, D_{gm}, D_{by}) +$ $\sum_{j=10+1}^{10+6} a_j 2^{nd} (D_{rc}, D_{gm}, D_{by}) +$ $\sum_{j=10+6+1}^{10+6+3} a_j 1^{st} (D_{rc}, D_{gm}, D_{by}) + 1$ $3^{rd} :$ $(a_1 D_{rc}^3 + a_2 D_{gm}^3 + a_3 D_{by}^3 + a_4 D_{rc}^2 D_{gm} + a_5 D_{rc}^2 D_{by} +$ $a_6 D_{gm}^2 D_{rc} + a_7 D_{gm}^2 D_{by} + a_8 D_{by}^2 D_{rc} + a_9 D_{by}^2 D_{gm} +$ $a_{10} D_{rc} D_{gm} D_{by})$ $2^{nd} :$ $(a_{11} D_{rc}^2 + a_{12} D_{gm}^2 + a_{13} D_{by}^2 + a_{14} D_{rc} D_{gm} + a_{15} D_{rc} D_{by} + a_{16} D_{gm} D_{by})$ $1^{st} :$ $(a_{17} D_{rc} + a_{18} D_{gm} + a_{19} D_{by} + a_{20})$
2 <sup>nd</sup> -SVD Equation (BB)	$D_{r3C}$ $D_{g3C}$ $D_{b3C}$ $D_{rKey}$ $D_{gKey}$ $D_{bKey}$	$(\sum_{i=0}^2 H_i^2) + 1 = 28$	$\sum_{j=1}^{C_2^7} a_j 2^{nd} (D_{r3C}, D_{g3C}, D_{b3C}, D_{rKey}, D_{gKey}, D_{bKey}) +$ $\sum_{j=C_2^7+1}^{C_2^7+C_2^6} a_j 1^{st} (D_{r3C}, D_{g3C}, D_{b3C}, D_{rKey}, D_{gKey}, D_{bKey}) + 1$
3 <sup>rd</sup> -SVD Equation (MB)	$R_{\lambda 1}$ $R_{\lambda 2}$ $R_{\lambda 3}$ $R_{\lambda 4}$	$(\sum_{i=0}^3 H_i^3) + 1 = 35$	$\sum_{j=1}^{C_3^6} a_j 3^{rd} (R_{\lambda 1}, R_{\lambda 2}, R_{\lambda 3}, R_{\lambda 4}) + \sum_{j=C_3^6+1}^{C_3^6+C_3^5} a_j 2^{nd} (R_{\lambda 1}, R_{\lambda 2}, R_{\lambda 3}, R_{\lambda 4}) +$ $\sum_{j=C_3^6+C_3^5+1}^{C_3^6+C_3^5+C_3^4} a_j 1^{st} (R_{\lambda 1}, R_{\lambda 2}, R_{\lambda 3}, R_{\lambda 4}) + 1$

Note: 1) BB: Broadband, MB: Multispectral; 2) ( $D_{r3c}, D_{g3c}, D_{b3c}$ ) and ( $D_{r4c}, D_{g4c}, D_{b4c}$ ) are the outcomes for both 3<sup>rd</sup>-SVD and 2<sup>nd</sup>-SVD equations respectively in broadband model ; 3)  $R_{\lambda 4c}$  is the outcome for 3<sup>rd</sup>-SVD equation in multispectral model.

and the 2<sup>nd</sup>-order with 3<sup>rd</sup>-order polynomial regression equations, incorporated with singular-value decomposition (SVD) technique (Press *et al.* 1992); and each carried out both the forward and the reverse

transform processes. The forward process maps the device-dependent data (i.e. FADs, Fractional Dot Areas of four primary inks for a color considered in each subset tested) to their device-independent values

(i.e. CIEXYZ, CIELAB, or CIELCH); while the reverse process transforms device-independent values (i.e. CIEXYZ, CIELAB, or CIELCH) into device-dependent data i.e. FDAs). The broadband type of 2<sup>nd</sup>-SVD model (referred as 2<sup>nd</sup>-SVD-BB later) was derived from previous work (Lo *et al.* 1997, 1998, 2006). As known in industry practice, consistency of color balance at all tone levels from white to black is quite important, and this requires close control of the relative response characteristics of both neutral and near-neutral color areas. Therefore in this work, a further modification was made on the reverse process of broadband model via using lightness-division approach (Lo *et al.* 2000) to enhance its predictive performance

As for the model developed based on the multispectral approach, it implemented using the 3<sup>rd</sup>-order polynomial regression equations (recognized as 3<sup>rd</sup>-SVD-MS later). Table 3 lists all the algorithms used in models derived. Only the whole set of polynomial forms for 3<sup>rd</sup>-SVD equation is demonstrated here to show the deriving process for different order of polynomial regression equations.

## Experimental

A printing device selected was Komori S40 press using 7-color printing process. The RIP (Raster Image Processor) chosen was HQ-510 Version 6.0., and incorporated with Randot X FM screening. A printing characterization data set of IT8.7/4 was used in this study as the training and test target. A GretagMacbeth SpectraScan spectrophotometer was used in the measurement, performed at 45/0 geometry of illuminating and viewing using CIE 1931 2<sup>o</sup> observer. Samples were taken over the range across the visible spectrum 380-730 nm with a 10 nm interval. The colorimetric data (i.e. device-dependent data of CIE XYZ, CIE LAB and CIE LCH) were obtained against CIE D<sub>50</sub> illuminant. The series of experimental steps are as follows:

- 1) Subdivide the 7-ink set into 7 subsets (see Table 1), each containing 3 chromatic inks plus black ink.
- 2) Generate the color training/test target for each of the sets of 4-ink grouping, using the 7-ink printing process.
- 3) Measure color patches in each target to obtain

spectral reflectance values, colorimetric data and device-dependent command (FDAs, fractional dot areas) values.

- 4) Construct both forward and reverse transform processes for each of the broadband and the spectra-based characterization models.
- 5) For every given color in each 4-ink grouping, attempt to process both forward and reverse transforms in each model derived (Figure 2).
- 6) Evaluate models performance in terms of 2 measures of Average (i.e. mean  $E^*_{00}$ ) and Max (i.e. maximum  $E^*_{00}$ ), tested using each subset of test targets ( $E^*_{00}$  is color difference of CIEDE2000).

$E^*_{00}$  was calculated between XYZ values of the predicted color-patch and those of the original target color-patch in question. Here, only the computational procedures used in both forward and reverse transforms for 3<sup>rd</sup>-SVD-MS model, based on the multispectral approach, will be described in Figure 2 since it is more complicated than that used in the broadband type of 2<sup>nd</sup>-SVD-BB model. As mentioned earlier, each of subgamuts, reproduced using the corresponding subset of 4-ink grouping, was individually characterized. The KRYG inkset will be used as an example to give demonstrations of computational procedures for both forward and reverse transforms of the 3<sup>rd</sup>-SVD-MS model.

For the forward transform (shown using  $\longrightarrow$ ) of 3<sup>rd</sup>-SVD-MS model, the FDAs of the KRYG inks are the input value. Then, those input data are first converted to their representative spectral reflectance (i.e.  $R_{\lambda 1}, R_{\lambda 2}, R_{\lambda 3}, R_{\lambda 4}$ ; here  $R_{\lambda 1} = R_{\lambda K}, R_{\lambda 2} = R_{\lambda R}, R_{\lambda 3} = R_{\lambda Y}, R_{\lambda 4} = R_{\lambda G}$ ) via plate-press look up table (LUT). Subsequently, the spectral reflectance (i.e.  $R_{\lambda 4C}$ ) of resultant 4-color overprint of KRYG is constructed via the 3<sup>rd</sup>-order regression equations. Consequently, the resultant tristimulus values of 4-color overprint can be accordingly computed against the CIE D50 illuminant.

In the reverse transform (shown using  $\longleftarrow$ ) of the spectrally-structured 3<sup>rd</sup>-SVD-MS model, the XYZ values (which are calculated from spectral reflectance) of a target color are first entered. Subsequently, the same algorithm, used in the reverse process of 2<sup>nd</sup>-SVD-BB by applying both the broadband and the lightness-division approaches as also shown in Figure

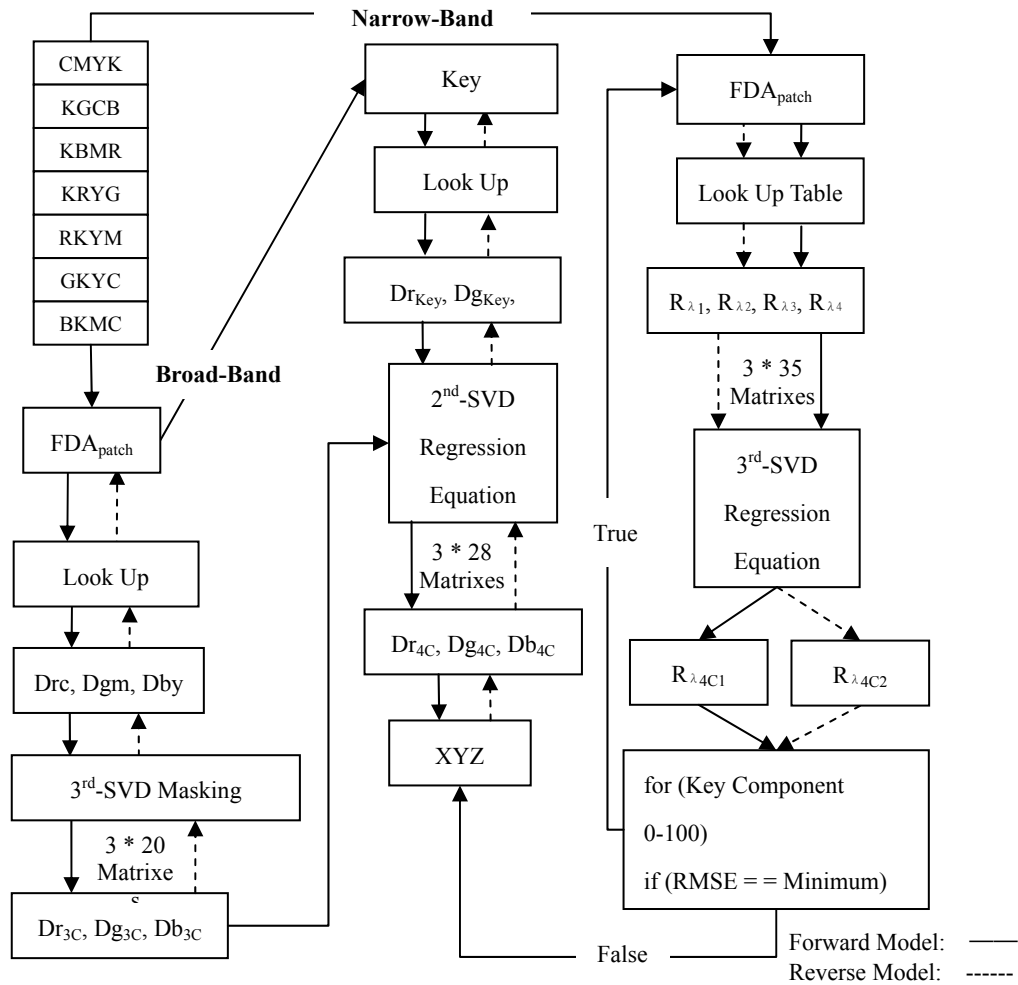


Figure 2. The computational procedures of both forward and reverse transforms used in the multispectral type of 3<sup>rd</sup>-SVD-MS model for characterizing 7-ink CMYKRGB printing process.

Models' Predictive Performances (Using CIE <sub>00</sub> Colour Difference)											
CMYK						KGCB					
Type	Broadband		Multispectral			Type	Broadband		Multispectral		
	F	R	F	R	RMSE		F	R	F	R	RMSE
Max	6.03	6.86	5.87	8.03	0.23	Max	4.52	7.49	8.11	6.14	0.21
Average	1.39	0.94	1.28	0.94	0.03	Average	0.77	0.59	0.91	0.68	0.02
KBMR						KRYG					
Type	Broadband		Multispectral			Type	Broadband		Multispectral		
	F	R	F	R	RMSE		F	R	F	R	RMSE
Max	6.15	7.18	7.78	9.52	0.20	Max	5.61	4.57	8.8	6.13	0.19
Average	1.06	0.96	1.03	0.99	0.03	Average	0.99	0.94	0.87	1.12	0.03
RKYM						GKYC					
Type	Broadband		Multispectral			Type	Broadband		Multispectral		
	F	R	F	R	RMSE		F	R	F	R	RMSE
Max	3.82	7.05	11.70	8.31	0.29	Max	3.30	3.18	4.75	4.97	0.12
Average	0.86	1.13	0.93	0.93	0.02	Average	0.71	0.70	0.70	0.77	0.02
BKMC						Global					
Type	Broadband		Multispectral			Type	Broadband		Multispectral		
	F	R	F	R	RMSE		F	R	F	R	RMSE
Max	2.98	4.54	8.21	8.71	0.19	Max	6.15	7.49	11.70	9.52	0.29
Average	0.88	0.88	0.96	0.92	0.03	Average	0.95	0.87	0.87	0.90	0.02

Table 3. Summary of models' predictive performances in both forward (F) and reverse (R) transform processes

2, was integrated into the forward transform of 3<sup>rd</sup>-SVD-MS model, to iteratively look for the optimal solution of printing device-dependent data (e.g. KRYG FDAs). In the optimization of iteration process, every possible solution of KRYG FDAs is input into the forward transform of 3<sup>rd</sup>-SVD-MS model to reconstruct the spectral reflectance of target color of interest in KRYG subgamut. Then, in terms of the measure of RMSE (root of mean square error), the best solution of KRYG-ink FDAs would be determined. The RMSE was computed between the iteratively recovered (i.e. predicted) spectra and original reference ones, of the target color, in the 36-dimensional (i.e. 36 spectral wavelengths) space.

## Results

The predictive performances of two models derived were tested using all the characterization data sets which were used to derive these models. As mentioned, two colorimetric measures of mean and maximum  $E^*_{00}$  calculated from all color samples in each of subset of 4-ink grouping, were used to evaluate models performances. For testing the forward transform of each model, for each color in each subset of 4-ink grouping, the  $E^*_{00}$  value was calculated between the measured XYZ values and its predicted XYZ values which were converted from the reconstructed spectral reflectance. The summary results are tabulated in Table 3.

For comparison of the reverse processes between two models, the XYZ tristimulus values of every color considered were first computed using predicted FDAs of 4 primary inks via their respective forward transform derived previously. Finally, details of two measures of Average (i.e. mean  $E^*_{00}$ ) and Max (i.e. maximum  $E^*_{00}$ ), used to define the reversibility performance, were obtained by comparing between those predicted and measured XYZ values. The results are also summarized in Table 3 for both of the 2<sup>nd</sup>-SVD-BB and the 3<sup>rd</sup>-SVD-MS models, in both forward and reverse transform processes. It is clearly shown that, two types of broadband and multispectral models performed similar, and gave satisfactorily pleasing results in both reverse and forward transform processes for each of 7 subgamuts, in terms of mean  $E^*_{00}$ . It can be seen that almost all the maximum  $E^*_{00}$

values for the multispectral model were a slightly bigger than those obtained from the broadband model in the reverse transform process. However, some errors in the multispectral model were resulted from both the integration of reverse form of the 3<sup>rd</sup>-SVD-BB model and the prediction variance of resultant XYZ values in the forward transform. Hence, it was considered that there were no big differences between these two models in terms of the maximum  $E^*_{00}$  values in the reverse transform since those errors should be neglected. Also in the forward transform process, as seen in some subgamuts, the broadband model seems performed a slightly better than the spectral one, also in term of the maximum  $E^*_{00}$  values. But, from the close comparisons between the reconstructed and the original spectral reflectance curves (e.g. Figure 3) of those data, which had large  $E^*_{00}$  values (especially samples having the maximum  $E^*_{00}$  values), it clearly showed that there were no marginally significant differences (RMSE is very small).

Figure 3 shows a very clear picture of the similarity between the original and the reconstructed spectral reflectance curves of three those samples selected from three of seven subgamuts. Moreover, with further looking into those colors, most of those data found are colors in very dark areas. Therefore, with the knowledge of human visual insensitivity to the shadow area of tones, those original and reproduced data, with very low lightness were visually very similar, and not considered to be significantly important to the prediction results.

## Conclusion

The research began with by taking two kernels of the matters of both “metamerism” and “gamuts” in mind, and intended to derive a universally well-performing Hi-Fi multi-color printing device characterization model. Therefore, the model derived would: 1) solve out metamerism problem to achieve the optimally requirement of color-matching independent of the illuminant; and 2) produce a color gamut that could approach those of displays (used for soft-proofing with high-rendition quality) or real dyes.

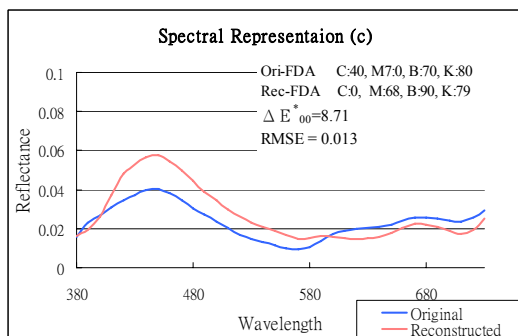
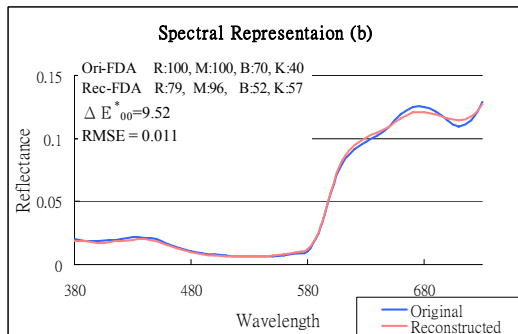
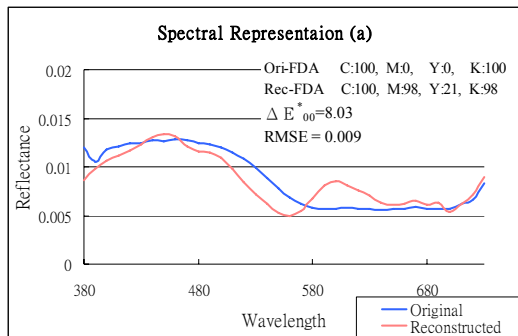


Figure 3. Comparisons between the original and the reconstructed spectral reflectance curves of 3 samples which have maximum  $E^*_{00}$  values selected from 3 of 7 subgamuts (Spectral Representations (a) to (c)).

Consequently, two types of printing characterization algorithms, used in the printing process of 7-ink CMYKRGB using FM screening technique, were successfully proposed. Those were 2<sup>nd</sup>-SVD-BB and 3<sup>rd</sup>-SVD-MS models, applying the 2<sup>nd</sup>-order and the 3<sup>rd</sup>-order with 2<sup>nd</sup>-order polynomial regression equations respectively, via the broadband and the multispectral approaches respectively. Satisfactorily, the broadband type could be used to perform a colorimetrically correct color-matching of color reproduction, but only under a specified illuminant considered. Since the 7-ink (heptatone) gamut approaches those of the film and high-quality display,

the broadband type could be also used to mitigate the problem of mapping unpredictable colors onto printable colors (i.e. gamut mapping). As for the multispectral one, it could be utilized in addition to extend color gamut in the Hi-Fi multi-color printing system; but also optimally reconstruct the spectral reflectance of colors in question to release the problem of color-matching dependent on illuminants.

The future work is to extend the 7-ink printing characterization models derived here by using LUT approach. Moreover, a set of psychophysical experiments will be conducted to deal with the visual differences between complex hardcopy of color images produced by models derived and their corresponding original (reference) images; and to compare the results with those obtained from the IT8.7/4 test-target experiments.

## Acknowledgements

This research has mainly supported by the National Science Council of Taiwan for financial assistance.

## References

1. Boll, H., A color to colorant transformation for a seven ink process. IS&T's Third Technical Symposium on Prepress, Proofing, & Printing, 3, 31-36 (1993).
2. Lo, M. C., Chen, C. L., Perng, R. K. and Hsieh, T. H., The characterisation of colour printing devices via physical, numerical and LUT models, CGIV 2006, IS&T's Third European Conference on Color in Graphics, Imaging, and Vision, University of Leeds, UK, 95-99 (2006).
3. Lo, M. C., Chiang, J.C., and Shi, L., Color separation for 7-ink printing using FM screening, TAGA proceeding, 716-735 (1997).
4. Lo, M. C., Perng, R. K. and Su, Y., An investigation of color medles'performacne between monitor and reflection image, TAGA proceeding (2000).
5. Lo, M.C. and Chiang, J. C., The characterization models for multi-colored CMYKRGB printing process, TAGA proceeding, 242-254 (1998).
6. Ostromoukhov, V., Chromaticity gamut

- enhancement by heptatone multi-color printing, IS&T/SPIE 1993 International Symposium on Electronic Imaging: Science & Technology, Proceedings Conf. Device-Independent Color Imaging and Imaging Systems Integration, SPIE, 1909, 139-151 (1993).
7. Press, W. H., Teukolsky, S. A., Vetterling, W. T., and Flannery, B., P., Numerical Recipes in C-The Art of Scientific Computing, 2<sup>nd</sup> edition, Cambridge University Press (1992).
  8. Son, C. H., Cho, Y. H., Park, K. H. and Ha, Y. H., Six color separation using the additional colorants with less dot visibility. Color Imaging Conference Final Program and Proceedings, 13, 189-194 (2005).
  9. Yule, J. A. C., Principles of Color Reproduction: Applied to Photomechanical Reproduction, Color Photography, and The Ink, Paper, and Other Related Industries. New York: John Wiley & Sons, Inc., 220-230 (1976).